Étude numérique des transferts thermiques dans les lits fluidisés : un nouveau fluide caloporteur pour les centrales solaires à concentration

Numerical study of heat transfer in fluidized bed: a new heat transfer fluid for Concentrated Solar Power

Alexandre LABAT[1,2], **Samuel MER**[1,2], **Françoise BATAILLE**[1,2], **Adrien TOUTANT**[1,2]

[1]Laboratoire PROMES-CNRS (UPR 8521), Perpignan, France
[2]Université de Perpignan Via Domitia (UPVD), Perpignan, France

Résumé - Afin d'améliorer l'efficacité solaire des centrales à tour de prochaines générations, la température cible en sortie de récepteur doit atteindre 800 °C. Les fluides caloporteurs actuels (huiles synthétiques ou sels fondus) ne permettent pas d'atteindre ces niveaux de température. Le laboratoire PROMES travaille depuis une dizaine d'années sur un concept de récepteur à lit fluidisé circulant dense, dans lequel un lit fluidisé d'air et de particules d'olivine fait office de fluide caloporteur. L'étude numérique de ces lits fluidisés chauffés a pour objectif de comprendre le comportement microscopique du système et, en particulier, les mécanismes de transfert thermique entre les parois, l'air de fluidisation et les particules. Les résultats montrent que les transferts thermiques sont principalement localisés à proximité des parois et qu'ils sont contrôlés par le temps de résidence des particules près des surfaces.

Résumé - In order to improve the efficiency of next-generation solar tower power plants, the target outlet temperature of the receiver must reach 800 °C. Current heat transfer fluids (synthetic oils or molten salts) do not allow such temperature levels. The PROMES laboratory has been working for about ten years on a concept of dense circulating fluidized-bed receiver, in which a fluidized bed of air and olivine particles acts as the heat transfer fluid. The numerical study of these heated fluidized beds aims to understand the microscopic behavior of the system and, in particular, the heat transfer mechanisms between the walls, the fluidizing air and the particles. The results show that the heat transfer is mainly localized near the walls and is controlled by the residence time of particles close to the surfaces.

Nomenclature

$\boldsymbol{u}$	velocity field, $\mathrm{m/s}$
T	temperature field, K
$\boldsymbol{g}$	gravity field, $\mathrm{m/s^2}$
ρ	density, $\mathrm{kg/m^3}$
μ	dynamic viscosities, $\mathrm{Pa\,s}$
λ	thermal conductivity, $\mathrm{W/(m\,K)}$
c_p	Thermal capacity, $\mathrm{J/(kg\,K)}$
p	pressure, Pa
α_p	particles fraction field
ε	emissivity
J	radiosity, $\mathrm{W/m^2}$
σ	Stefan–Boltzmann law, $\mathrm{W/(m^2\,K^4)}$
F	view factor
S_p	particle surface, $\mathrm{m^2}$
V_p	particle volume, $\mathrm{m^3}$
Φ, $\dot{Q}$	heat flux, W
$_\mathrm{p}$, $_\mathrm{f}$	particle and fluid subscripts
Δx	mesh element size, m
d_p	particle diameter, m
m_p	particle mass, kg

https://doi.org/10.25855/SFT2026-062

1. Introduction

Gas-solid fluidized beds have long been used as efficient heat exchangers due to their ability to transport heat with a nearly uniform temperature distribution [17]. The intense mixing of particles induced by fluidization enhances wall-to-bed heat transfer coefficients, which are significantly higher than those obtained with single-phase gas flows [17, 19].

Recent studies have highlighted the potential of dense particle suspensions and fluidized beds as heat transfer fluids in Concentrated solar power (CSP) systems [10, 9]. Their ability to operate at high temperatures opens perspectives for advanced thermodynamic cycles, including supercritical steam and supercritical carbon dioxide power cycles and is what's motivate this work. High-temperature fluidized beds are therefore considered as a viable alternative to conventional heat transfer fluids for both heat transport and thermal energy storage in solar tower technologies [11].

Heat transfer between a fluidized bed and confining walls is governed by the formation of thin thermal boundary layers. Compared to single-phase flows, these boundary layers are significantly thinner due to particle–fluid interactions and locally increased interstitial velocities near the wall [17, 16, 22, 24]. These thin boundary layers prevent the fluid to act as an insulating layer, thus increasing the overall heat transfer coefficient [8]. Experimental studies indicate that the effective thickness of the wall boundary layer is of the same order of length then particle diameter [7, 24]. Furthermore, the residence times of particle near the wall determine how fast particles can drain heat of the walls. Recent studies decompose the wall-to-bed heat transfer coefficient into particle convection, fluid convection, and radiation contributions [11]. At low temperatures, particle convection dominates, while fluid convection and radiation become increasingly important at higher temperatures.

The wall-to-bed heat transfer coefficient depends strongly on the fluidization regime and operating conditions. It has been reported that heat transfer is lower near the bed inlet, where particle mixing is poorer, and increases toward the top of the bed [17]. Furthermore, when the fluidization regime is turbulent, the wall-to-bed heat exchange is maximized [13, 14]. This effect can be explained by noting two competing phenomena: on one hand circulation promotes intense particle mixing, preventing the development of stable temperature profiles near the wall and thus mechanically increasing the local temperature gradient and heat transfer coefficient. On the other hand, the formation and upward propagation of start-up bubbles reduce the local solid concentration near the wall, decreasing the effective heat transfer [19]. Increasing pressure also enhances heat transfer by inducing a more homogeneous fluidization [17].

Beyond the heat transfer maximization goal, the strong heterogeneity of solid volume fraction near confining walls, combined with the high temperatures encountered in CSP receivers, leads to spatially non-uniform temperature gradients. This non-uniformity induce thermomechanical stresses in receiver walls, reducing the life span of CSP receiver [6]. Thus, characterizing heat transfer near the walls of fluidized-bed solar receivers supports the development of CSP infrastructures that are both thermally efficient and resistant to long-term thermal stresses.

Experimental studies of fluidized bed in CSP receiver give only partial access to heat transfer mechanism. Indeed, the particle size ($70\,\mu\mathrm{m}$) is too small to be able to fully capture heat transfer at the particle size with current measuring tools. For this reason, detailed experiments on fluidized bed hydrodynamic – like the one reported by Aguilar-Corona, Zenit, and Masbernat [1] and Alméras et al. [2] – use particles of a few millimeters in diameter. Furthermore, for the specific case of CSP applications, most materials capable of withstanding the thermal constraints imposed by the concentrated solar flux on the receiver are opaque and therefore do not allow optical access to the two-phase flow inside the receiver. For these reasons, the present study aims to analyze the heat transfer mechanisms using a numerical simulation approach, allowing more precise insights into particle behavior in fluidized-bed-based heat transfer.

2. Numerical method

The numerical method presented here has been implemented in the version `1.9.6` of `TrioCFD` , an open source high performance computing code developed by the CEA.

2.1. Two-phase flow solver

The particulate phase is composed of rigid, non-deformable particles. To align with previous experimental and numeric studies, all particles are assumed to be perfectly spherical and monodisperse, *i.e.* they share the same diameter. To reduce the computational cost, the carrier fluid is considered incompressible, and its thermophysical properties are assumed to be constant. Each particle is assumed to have a homogeneous internal temperature, which is justified by the high thermal conductivity of the solid phase and the relatively small particle size. Furthermore, thermal expansion of the particles is neglected. Particle–particle collisions are modelled using a soft-sphere approach [15]. Due to the high rigidity of the particles, deformations during collisions are neglected.

Direct numerical simulations are performed using a one-fluid formulation of the Navier–Stokes and energy equations. In this framework, both fluid and particle phases are described on a single computational domain discretized with an Eulerian mesh. The local hydrodynamic properties (in a mesh cell), such as viscosity and density, vary depending on a phase indicator function – indicating the proportion of each phase in this cell. A significant viscosity ratio between fluid and particles is imposed (usually taken as $\mu_{\mathrm{p}} = 10^4\mu_{\mathrm{f}}$) to enforce particle rigidity and prevent deformation.

One-fluid formulation of both Navier-Stokes and energy is as follows

- Conservation equation:

$$\boldsymbol{\nabla} \cdot \boldsymbol{u} = 0 \tag{1}$$

- Momentum equations:

$$\frac{\partial \rho \boldsymbol{u}}{\partial t} + \boldsymbol{\nabla} \cdot (\rho \boldsymbol{u} \otimes \boldsymbol{u}) = -\boldsymbol{\nabla} \boldsymbol{p} + \boldsymbol{\nabla} \cdot \left[\mu \left(\boldsymbol{\nabla} \boldsymbol{u} + (\boldsymbol{\nabla} \boldsymbol{u})^{\mathsf{T}}\right)\right] + \rho \boldsymbol{g} + \boldsymbol{F_c^E} \tag{2}$$

  with $\boldsymbol{F_c^E}$ the force term induced by collisions between particles and between particles and walls.

- Energy equation:

$$\frac{\partial}{\partial t}(\rho_{\mathrm{f}} c_p T) + \boldsymbol{\nabla} \cdot (\rho_{\mathrm{f}} c_p \boldsymbol{u} T) = \boldsymbol{\nabla} \cdot (\lambda_{\mathrm{f}} \boldsymbol{\nabla} \boldsymbol{T}) \tag{3}$$

Fluid density and viscosity [18, 20], are locally evaluated using the solid fraction field α_{p}

$$\rho = \alpha_{\mathrm{p}}\rho_{\mathrm{p}} + (1-\alpha_{\mathrm{p}})\rho_{\mathrm{f}} \tag{4}$$

$$\mu = \frac{\mu_{\mathrm{f}}\mu_{\mathrm{p}}}{(1-\alpha_{\mathrm{p}})\mu_{\mathrm{p}} + \alpha_{\mathrm{p}}\mu_{\mathrm{f}}} \tag{5}$$

The particle surfaces are represented using a moving, triangle-based surface mesh, referred to as *Lagrangian* in the following. This mesh evolves in time to track particle motion and is used to reconstruct the phase distribution at each time step, following a front-tracking methodology [21]. This approach enables an accurate description of fluid–particle interfaces while preserving sharp phase boundaries over time. Coupling between the Eulerian and Lagrangian mesh is assure by the $\boldsymbol{F_c^E}$ force term in Navier-Stokes equations 2 and the velocity field: The force term allows the Lagrangian mesh to influence fluid motion during a collision and the velocity field is used in an interpolation to estimate the movement of the particles over time.

2.2. Heat transfer calculation

The Biot number of particles in a fluidized bed can be expressed as $\mathrm{Bi} = \mathrm{Nu}\,\lambda_\mathrm{f}/\lambda_\mathrm{p}$. For typical gas–solid systems, the ratio between fluid and particle thermal conductivities is small. Furthermore, Nusselt correlations at minimum fluidization and in turbulent regime indicate that the Nusselt stays close to 2 [24, 5, 23, 17]. As a result, the $\mathrm{Bi} \ll 1$ indicating that particles can be modeled as isothermal bodies, simplifying the calculation procedure.

At the particles surface, the temperature boundary condition is imposed using a ghost-fluid approach [12]. The energy equation is solved over the entire domain considering the fluid thermo-physical properties. However, the native approach implemented in `TrioCFD` does not allow the particles' temperature to evolve over time. To do so, we evaluate the heat flux received by each particle, thanks their local Eulerian temperature field, to compute the particle temperature evolution via the following energy balance

$$T_\mathrm{p}{}^{t+\Delta t} = T_\mathrm{p}{}^{t} + \frac{\dot{Q}_\mathrm{p}}{m_\mathrm{p} c_{p_\mathrm{p}}} \Delta t,\; \dot{Q}_\mathrm{p} = \Phi_\mathrm{p} = \Phi_\mathrm{p}{}^{\mathrm{conductive}}. \tag{6}$$

To compute the conductive heat flux, a preliminary study has shown that instead of interpolating the temperature gradient around a particle on the Lagrangian mesh [4, 3], one should instead integrate the temperature laplacian over all cells belonging to a given particle, which can be expressed as

$$\Phi_\mathrm{p}{}^{\mathrm{conductive}} = \iiint\limits_{V_\mathrm{p}} \lambda_\mathrm{f} \nabla^2 T \mathrm{d}V \tag{7}$$

where V_p covers all solid and mixed fluid-solid eulerian cells. To determine which Eulerian cells belong to a given particle, we compute solid cells connected components, assuming that closely spaced particles are always separated by at least one layer of mixed fluid-solid cells. These mixed cells are then assigned to a specific particle by tracing the path from their initial position toward the neighboring cells with the highest solid fraction.

Preliminary simulations showed that, while the method described above accurately predicts conductive and convective heat fluxes for a stationary, single-particle case, discrepancies arise in multi-particle non-stationary cases. To ensure energy conservation, the conductive heat flux can be corrected using the total heat flux entering the particles $\sum_i \Phi_i$, the total heat flux at the walls, and the unsteady energy term associated with temperature fluctuations in the fluid phase, whose magnitude is assumed to be linearly correlated with the conductive heat flux.

$$\Phi_\mathrm{p}{}^{\mathrm{corrected}} = \frac{\Phi_\mathrm{p}}{\sum_i \Phi_i} \left(\Phi_{\mathrm{walls}} - \sum_f m_\mathrm{f} c_{p_\mathrm{f}} \frac{\partial T}{\partial t} \right) \tag{8}$$

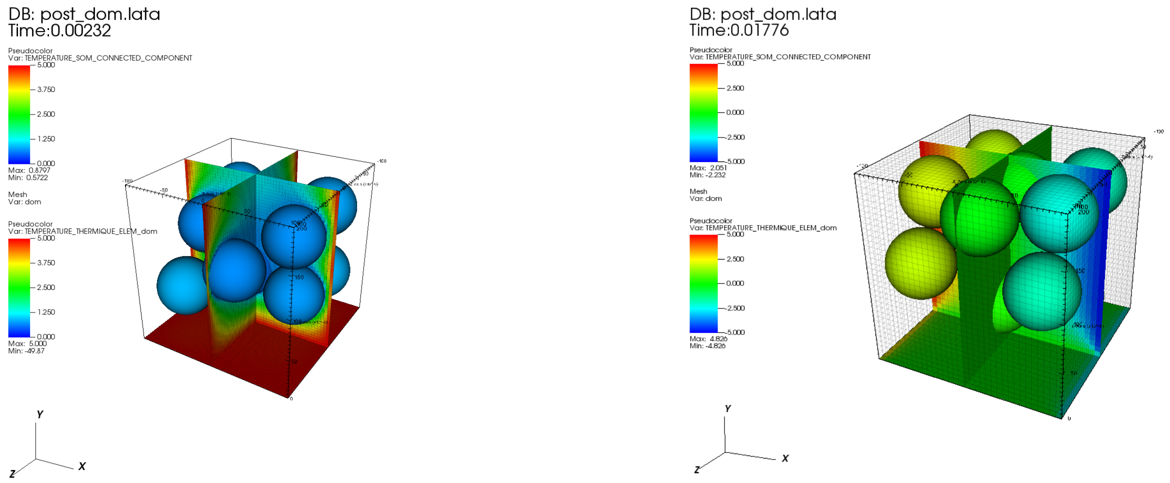

(a) Temperature convergence of particles initially at 0 °C with walls temperature at 5 °C.

(b) Temperature convergence of particles initially at 0 °C with walls temperatures at ±5 °C *gradient.*

Figure 1 : *Heated fluidized bed preliminary simulation. The particles temperature converge to the local mean temperature of the fluid.*

which guarantees that $\sum \Phi_{\mathrm{p}}{}^{\mathrm{corrected}} = \Phi_{\mathrm{walls}} - \sum_{\mathrm{f}} m_{\mathrm{f}} c_{p\mathrm{f}} \frac{\partial T}{\partial t}$. Figure 1 shows thermal behavior of particles in non-uniform heated fluidized bed.

3. Results

3.1. Single particle case study

Simulations have been conducted to evaluate the validity of heat transfer computation from the fluid to the particles at different resolution. Comparing the computed heat transfer without applying the correction given by equation 8 to the wall heat transfer allows the accuracy of the method to be assessed. From Figure 2b, the resulting error is estimated to be below $0.1\,\%$ for any resolution.

3.2. Multi-particles case study

Following this single-particle validation of the methodology, four different configurations of gas–particle fluidized-bed are investigated. Their properties are summarized in Table 1. These configurations are adapted from the work of Butaye (see Chapter 5 of [4]) to be representative of gas–particle flows in solar receivers. To this end, the particle properties are set to those of olivine [14]. The fluidizing gas stream is defined using the properties of air at $20\,°\mathrm{C}$.

The particles have a radius of $d_{\mathrm{p}} = 70\,\mu\mathrm{m}$. The thermal configuration is defined to impose a thermal disequilibrium around a reference temperature T_{ref} Within this framework, the particles are initially at T_{ref}, as is the incoming fluidizing gas. A symmetric thermal disequilibrium is imposed on two of the four side walls, with one wall set to $T_{\mathrm{ref}} + 10\,°\mathrm{C}$ and the opposite wall set to $T_{\mathrm{ref}} - 10\,°\mathrm{C}$. The two remaining walls, as well as the outlet temperature, are maintained at T_{ref}.

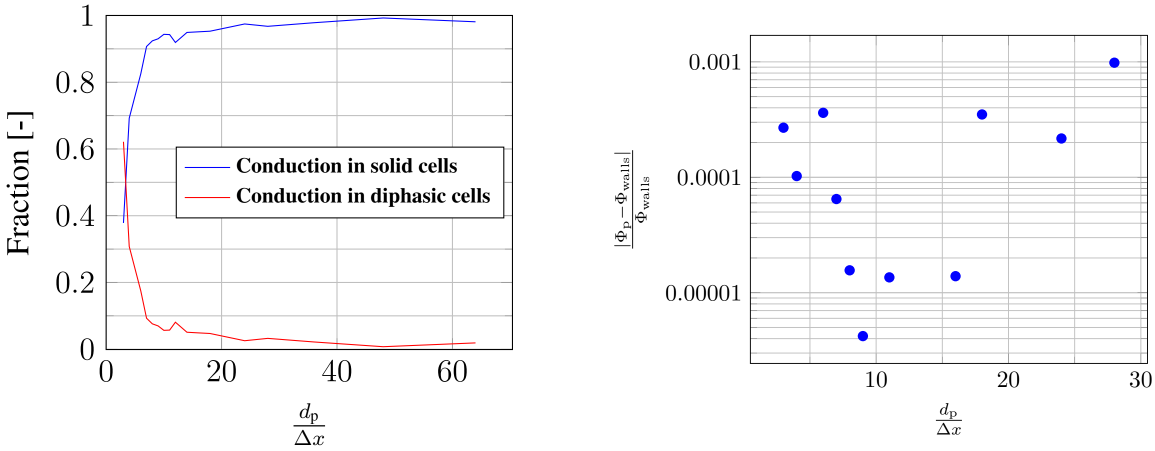

(a) Heat flux decomposition on a single particle for different mesh resolution. Fraction evaluated as $\%_{X_i} = \frac{|X_i|}{\sum |X_j|}$.

(b) Error heat flux computed at the boundaries of the domain and heat flux at from the fluid to the particle. In this stationary case the particle heat flux should equal the wall heat flux.

Figure 2 : *Evaluation of heat transfer in a single particle stationary configuration for different mesh resolution* $\frac{d_p}{\Delta x}$. *The fluid is air at ambient temperature and solid is olivine.* $d_p = 70\,\mu\text{m}$.

Table 1 : *Fluidized-beds properties*

	Inlet velocity [mm/s]	Number of particles	Size
1	13	2134	$(0.84 \times 1.89 \times 0.84)\,\text{mm}^3$
2	26	2134	$(0.84 \times 1.89 \times 0.84)\,\text{mm}^3$
3	52	2134	$(0.84 \times 4.62 \times 0.84)\,\text{mm}^3$
4	52	4268	$(0.84 \times 7.56 \times 0.84)\,\text{mm}^3$
5	52	17072	$(1.68 \times 7.56 \times 1.68)\,\text{mm}^3$

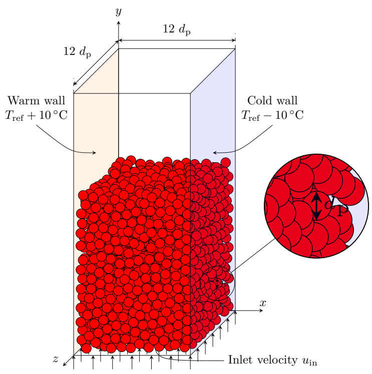

Figure 3 : *Configuration of the fluidized-bed simulations.*

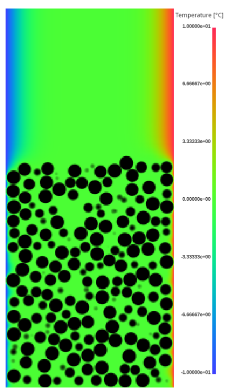

Figure 4 : *Temperature field near the start of the simulation.*

The five configurations differ in inlet gas velocity in order to investigate the effect of changes in the fluidization regime on heat transfer. The fifth case double the base dimensions in order to limit unwanted boundary effects. The height of the simulation domain is adjusted accordingly to accommodate the increase in bed expansion with increasing fluidization velocity. Simulations are currently under process.

4. Conclusion

A numerical method has been developed to study heat transfer in a heated fluidized bed under air–olivine conditions. A method for evaluating heat transfer from the temperature field was implemented and demonstrated sufficient accuracy in predicting particle temperature evolution over time. Simulations involving larger numbers of particles are currently underway to further investigate heat transfer in fluidized bed.

References

[1] A. Aguilar-Corona, R. Zenit, and O. Masbernat. "Collisions in a Liquid Fluidized Bed". In: *International Journal of Multiphase Flow* 37.7 (Sept. 1, 2011), pp. 695–705. ISSN: 0301-9322.

[2] E. Alméras, O. Masbernat, F. Risso, and R. O. Fox. "Fluctuations in Inertial Dense Homogeneous Suspensions". In: *Physical Review Fluids* 4.10 (Oct. 16, 2019), p. 102301. ISSN: 2469-990X.

[3] E. Butaye, R. Quintana, S. Mer, F. Bataille, and A. Toutant. "Investigation of Heat Transfers with Particle-Resolved Simulations: From Stokes Flow to Fluidized Bed". In: *International Journal of Heat and Mass Transfer* 241 (May 15, 2025), p. 126687. ISSN: 0017-9310.

[4] E. Butaye. "Modélisation et Simulations Résolues d'écoulement Fluide-Particules : Du Régime de Stokes Aux Lits Fluidisés Anisothermes". These de doctorat. Perpignan, Dec. 9, 2024.

[5] *Chemical Engineering Volume 1*. Oct. 19, 1999. ISBN: 978-0-08-050101-7.

[6] Y. Deng, A. Le Gal, E. Guillot, G. Flamant, and J. Baeyens. "Particle Conveyance in a Particle-driven CSP Loop: Design, Operation, Attrition and Erosion". In: *E3S Web of Conferences* 643 (Aug. 29, 2025).

[7] F. Di Natale, A. Lancia, and R. Nigro. "A Single Particle Model for Surface-to-Bed Heat Transfer in Fluidized Beds". In: *Powder Technology* 187.1 (Oct. 8, 2008), pp. 68–78. ISSN: 0032-5910.

[8] G. Flamant, N. Fatah, and Y. Flitris. "Wall-to-Bed Heat Transfer in Gas—Solid Fluidized Beds: Prediction of Heat Transfer Regimes". In: *Powder Technology* 69.3 (Mar. 1, 1992), pp. 223–230. ISSN: 0032-5910.

[9] G. Flamant et al. "A New Heat Transfer Fluid for Concentrating Solar Systems: Particle Flow in Tubes". In: *Energy Procedia* 49 (2014), pp. 617–626. ISSN: 18766102.

[10] G. Flamant et al. "Dense Suspension of Solid Particles as a New Heat Transfer Fluid for Concentrated Solar Thermal Plants: On-Sun Proof of Concept". In: *Chemical Engineering Science* vol. 102 (Oct. 2013), pp. 567–576.

[11] G. Flamant et al. "Opportunities and Challenges in Using Particle Circulation Loops for Concentrated Solar Power Applications". In: *Progress in Energy and Combustion Science* 94 (Jan. 1, 2023), p. 101056. ISSN: 0360-1285.

[12] M. Grosso, G. Bois, and A. Toutant. "Thermal Boundary Layer Modelling for Heat Flux Prediction of Bubbles at Saturation: *A Priori* Analysis Based on Fully-Resolved Simulations". In: *International Journal of Heat and Mass Transfer* 222 (May 1, 2024), p. 124980. ISSN: 0017-9310.

[13] R. Gueguen et al. "Gas-Solid Flow in a Fluidized-Particle Tubular Solar Receiver: Off-Sun Experimental Flow Regimes Characterization". In: *Energies* 14.21 (21 Jan. 2021), p. 7392. ISSN: 1996-1073.

[14] R. Gueguen et al. "Heat Transfer in a Fluidized Bed Tubular Solar Receiver. On-sun Experimental Investigation". In: *Solar Energy* 265 (Nov. 15, 2023), p. 112118. ISSN: 0038-092X.

[15] M. S. Hamidi, A. Toutant, S. Mer, and F. Bataille. "Assessment of a Coupled VOF-Front-Tracking/DEM Method for Simulating Fluid–Particles Flows". In: *International Journal of Multiphase Flow* 165 (Aug. 1, 2023), p. 104467. ISSN: 0301-9322.

[16] A. R. Khan and A. Elkamel. "Mathematical Model for Heat Transfer Mechanism for Particulate System". In: *Applied Mathematics and Computation* 129.2 (July 10, 2002), pp. 295–316. ISSN: 0096-3003.

[17] "Butterworth–Heinemann Series in Chemical Engineering". In: *Fluidization Engineering (Second Edition)*. Ed. by D. Kunii and O. Levenspiel. Boston: Butterworth-Heinemann, Jan. 1, 1991, p. ii. ISBN: 978-0-08-050664-7.

[18] J. Magnaudet, H. Bruhier, S. Mer, and T. Bonometti. "Rational Constitutive Law for the Viscous Stress Tensor in Incompressible Two-Phase Flows: Derivation and Tests against a Three-Dimensional Benchmark Experiment". In: *Physical Review Fluids* 10.7 (July 18, 2025), p. 074001.

[19] M. Syamlal and D. Gidaspow. "Hydrodynamics of Fluidization: Prediction of Wall to Bed Heat Transfer Coefficients". In: *AIChE Journal* 31.1 (1985), pp. 127–135. ISSN: 1547-5905.

[20] A. Toutant. "Viscous Stress Modeling for One-Fluid Approach in Newtonian Two-Phase Flows". In: *Physics of Fluids* 37.2 (Feb. 1, 2025). ISSN: 1070-6631.

[21] S. O. Unverdi and G. Tryggvason. "A Front-Tracking Method for Viscous, Incompressible, Multi-Fluid Flows". In: *Journal of Computational Physics* 100.1 (May 1, 1992), pp. 25–37. ISSN: 0021-9991.

[22] X. S. Wang and M. J. Rhodes. "Determination of Particle Residence Time at the Walls of Gas Fluidized Beds by Discrete Element Method Simulation". In: *Chemical Engineering Science* 58.2 (Jan. 1, 2003), pp. 387–395. ISSN: 0009-2509.

[23] J. G. Yates and P. Lettieri. *Fluidized-Bed Reactors: Processes and Operating Conditions*. Vol. 26. Particle Technology Series. Cham: Springer International Publishing, 2016. ISBN: 978-3-319-39591-3 978-3-319-39593-7.

[24] H. Zhang, J. Degrève, J. Baeyens, and R. Dewil. "Wall-to-Bed Heat Transfer at Minimum Gas-Solid Fluidization". In: *Journal of Powder Technology* 2014 (Sept. 17, 2014).

Acknowledgements The authors acknowledge GENCI and the TGCC for access to the computational resources used in this study (allocation A0182B11441 – $14 \times 10^6\ \mathrm{h_{CPU}}$**) and the CEA for usage of TRUST/TrioCFD software.**